

Metastasis-related *in vitro* assays and *in vivo* xenograft models



WuXi Biology, Oncology & Immunology Unit



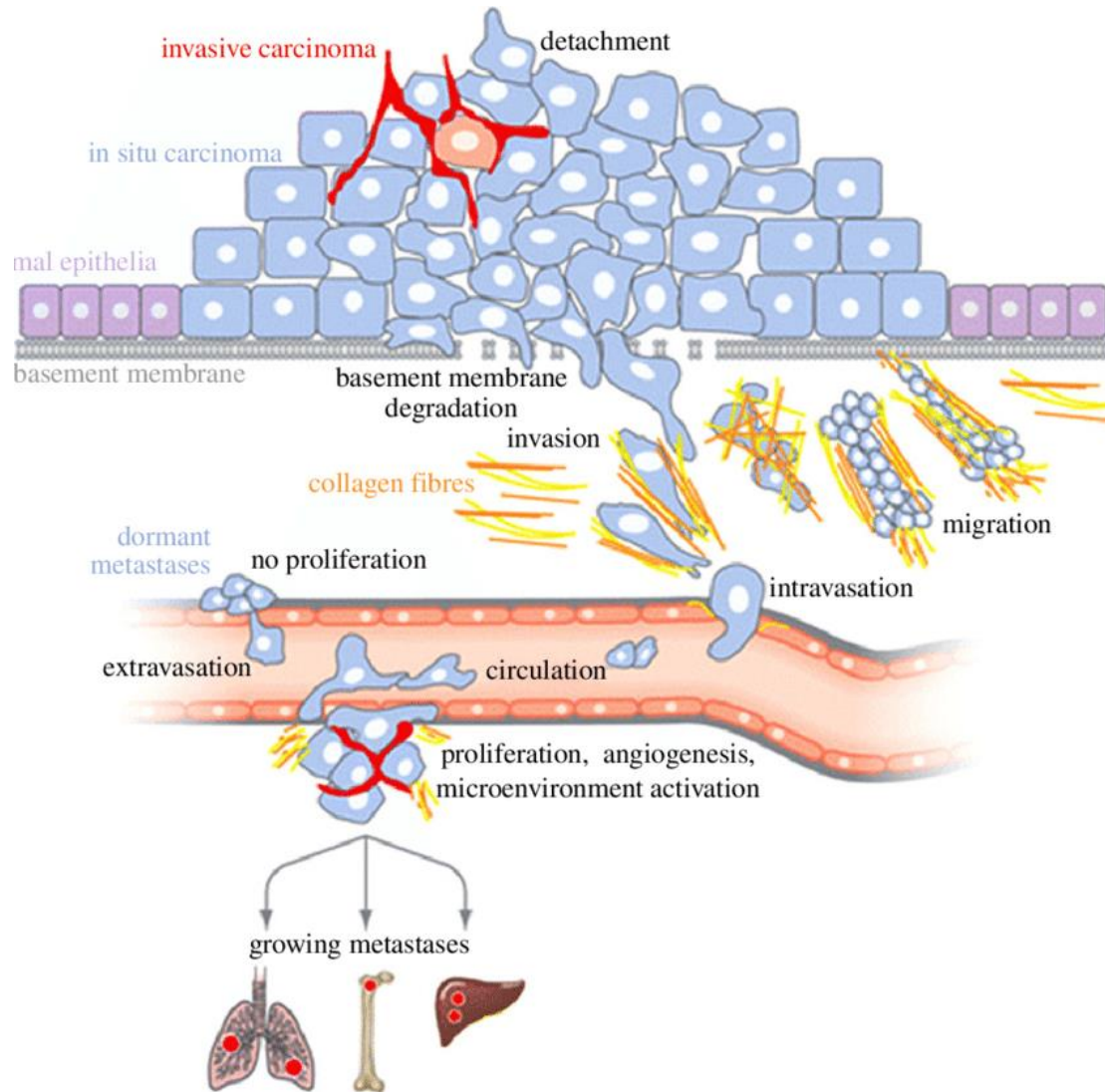
2023.08

OncoWuXi Newsletter

Outline

- Introduction of cancer metastasis
 - Cancer metastasis related *in vitro* assays
- Transwell migration assay
 - Transwell invasion assay
- Experimental metastasis xenograft models
 - Brain metastasis xenograft models
 - Bone metastasis xenograft models
 - Liver metastasis xenograft models
 - Disseminated metastasis xenograft models
 - Organ-specific metastasis models established by *in vivo* selection

Introduction of cancer metastasis

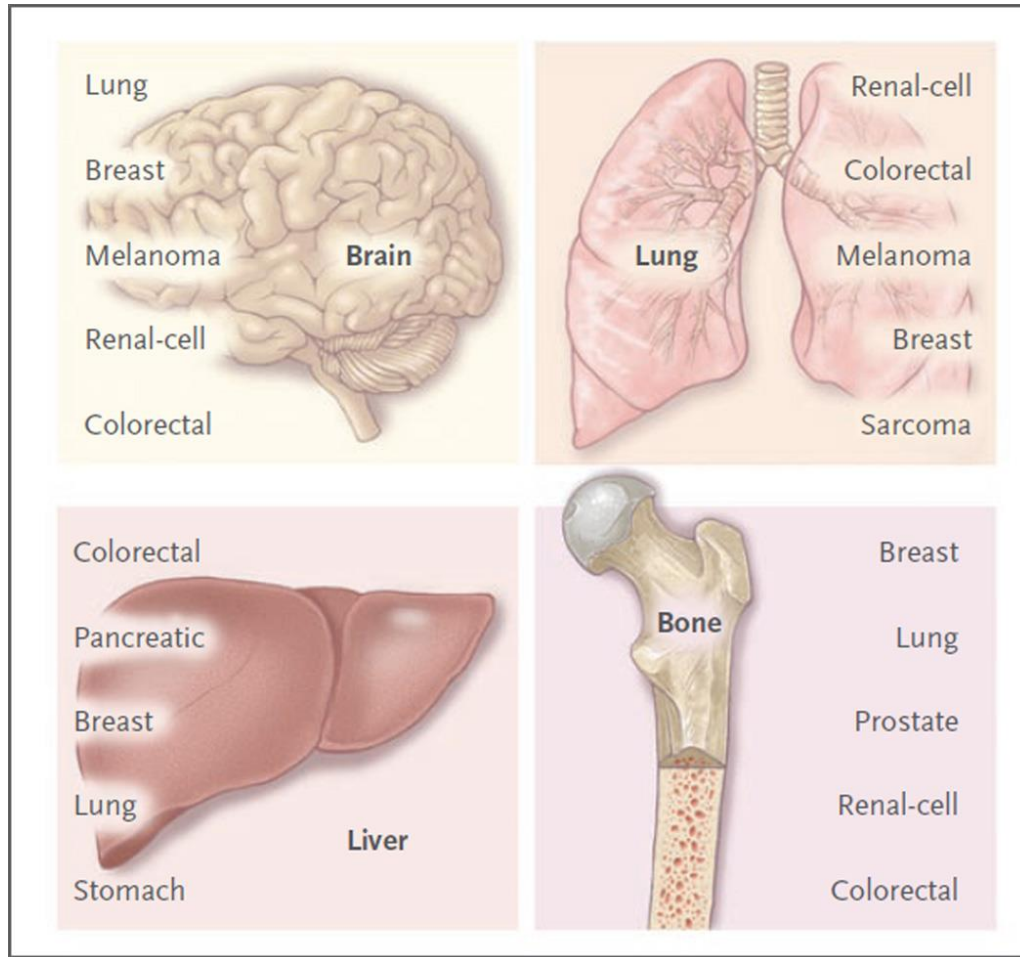


- Cancer metastasis, which accounts for most deaths due to malignancies, is an organ-selective and multi-stepping process that is started by escape of tumor cells from the primary tumor and ended with colonizing secondary tumors in the distant sites. This process involves the complex interplay of tumor and host intrinsic factors.
- Cancer cells disseminating from a primary tumor via the blood or lymphatic system require specific functions to adapt to a number of stresses in order to invade vessels, survive the loss of niche factors from the originating organ and survive in the circulation. On reaching distant organs, cancer cells enter and exit proliferative dormancy, evade immunity and acquire mitogenic signals by co-opting the stroma of the distant organs.

Philos Trans R Soc Lond B Biol Sci. 2014 Feb 3;369(1638):20130092.

Common sites of cancer metastasis

Cancer can spread to almost any part of the body, although different types of cancer are more likely to spread to certain areas than others. The organs mostly affected by metastases are lung, liver, brain and bone.



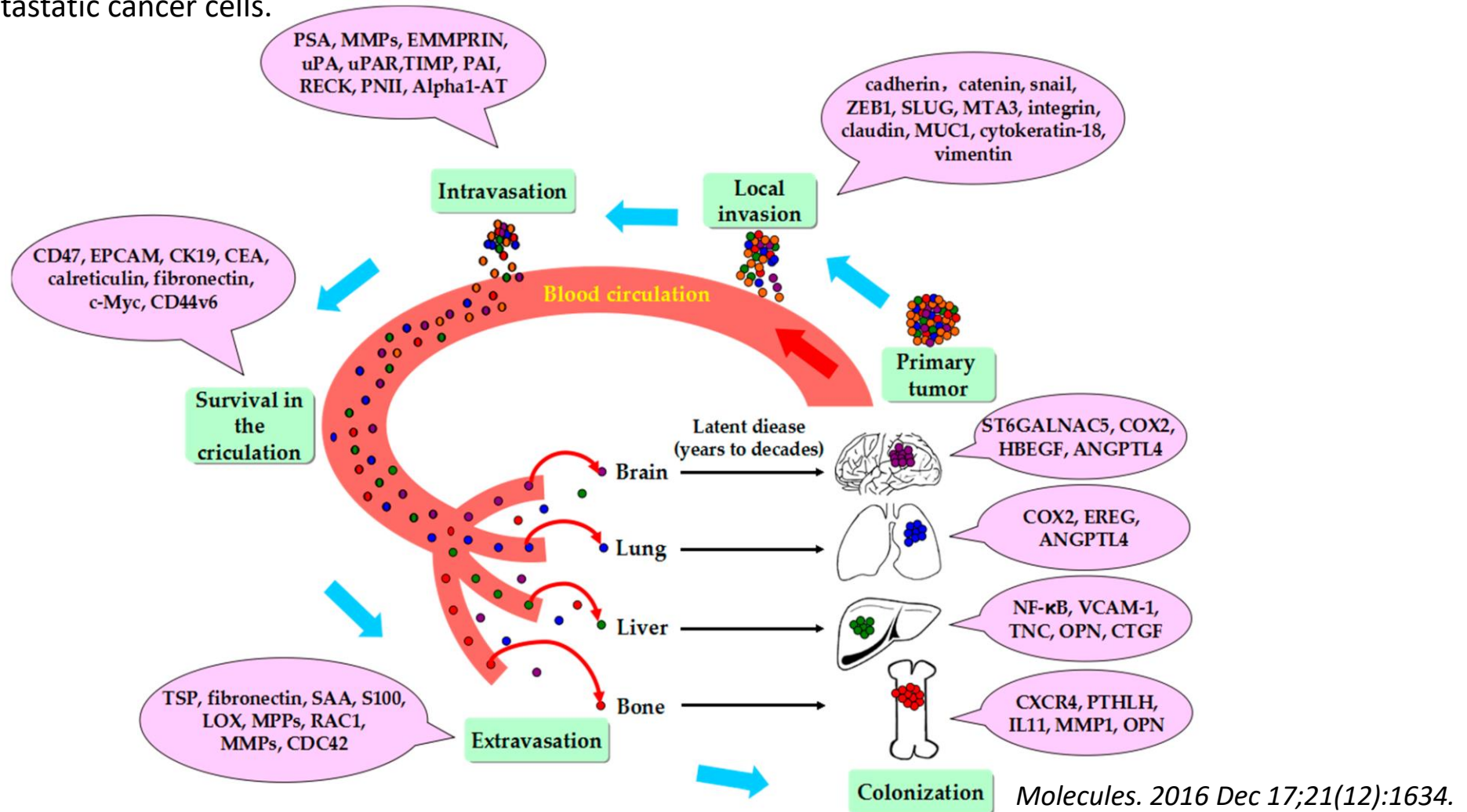
Cancer Type	Main Sites of Metastasis
Bladder	Bone, liver, lung
Breast	Bone, brain, liver, lung
Colon	Liver, lung, peritoneum
Kidney	Adrenal gland, bone, brain, liver, lung
Lung	Adrenal gland, bone, brain, liver, other lung
Melanoma	Bone, brain, liver, lung, skin, muscle
Ovary	Liver, lung, peritoneum
Pancreas	Liver, lung, peritoneum
Prostate	Adrenal gland, bone, liver, lung
Rectal	Liver, lung, peritoneum
Stomach	Liver, lung, peritoneum
Thyroid	Bone, liver, lung
Uterus	Bone, liver, lung, peritoneum, vagina

N Engl J Med 2008; 359:2814-2823

<https://www.cancer.gov/types/metastatic-cancer>

Molecular mechanisms of metastasis

The interrelated and sequential multi-steps of metastasis require certain transformations of cancer cells at each step, from primary site to metastatic site. Numerous genes and molecules have been implicated into this dynamic and adaptable evolution of metastatic cancer cells.



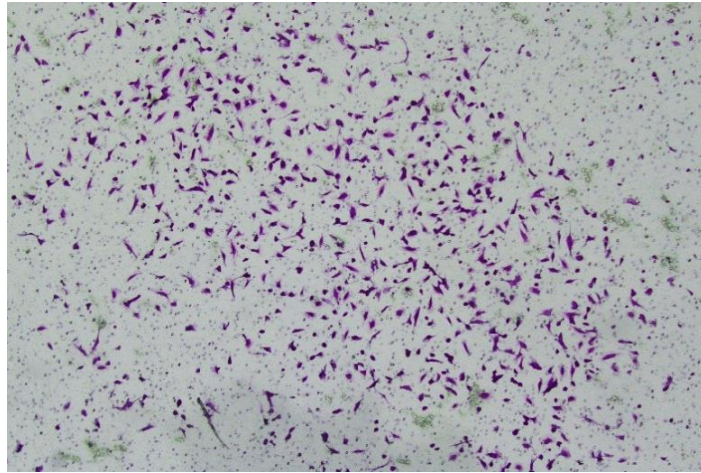
Transwell Migration and Invasion Assays

- Cell migration, invasion, and adhesion are pivotal steps in cancer metastasis. Transwell migration and invasion assay are widely-used *in vitro* assays to assess cell migratory behavior.
- The transwell migration assay measures the chemotactic capability of cells toward a chemo-attractant. The transwell invasion assay, however, measures both cell chemotaxis and the invasion of cells through extracellular matrix, a process that is commonly found in cancer metastasis or embryonic development.

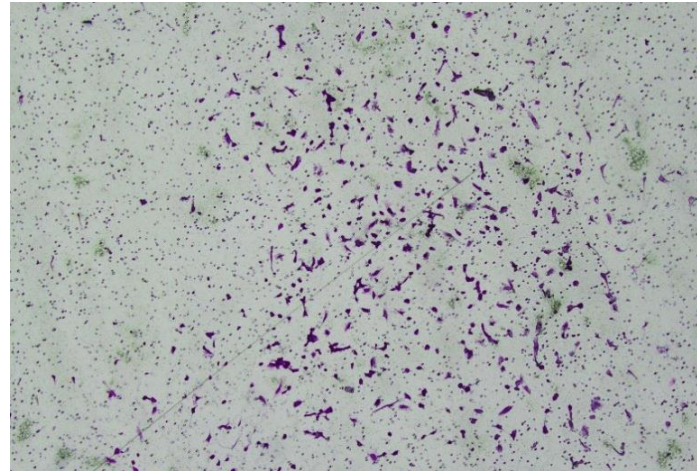
Assay	Definition	Cell type	Pore Size	Insert coating
Migration	chemotaxis Migration of cells toward a chemoattractant (chemical signal) in the cell's surrounding environment	Neutrophils Leukocytes	3 μm	None
		Lymphocytes Monocytes Macrophages	5 μm	None
		Fibroblasts, Endothelial Cells, Epithelial Cells, Tumor Cells	8 μm	None
		Astrocytes Slow-moving Cells	12 μm	None
	hap-totaxis Migration of cells along a gradient of cellular adhesion sites or extracellular matrix-bound chemoattractants	Fibroblasts Endothelial Cells Epithelial Cells	8 μm	Collagen I (bottom) Fibronectin (bottom)
Invasion	Movement of cells through the 3D extracellular matrix into neighboring tissues; includes ECM degradation and proteolysis	Fibroblasts, Endothelial Cells, Epithelial Cells, Tumor Cells	8 μm	ECM Matrix (top) Collagen I (top) Laminin I (top)

Transwell Migration Assay

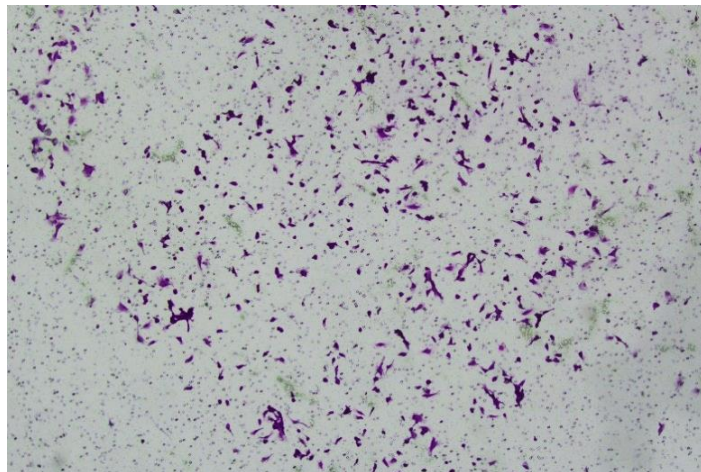
Case study: HUVEC cell migration



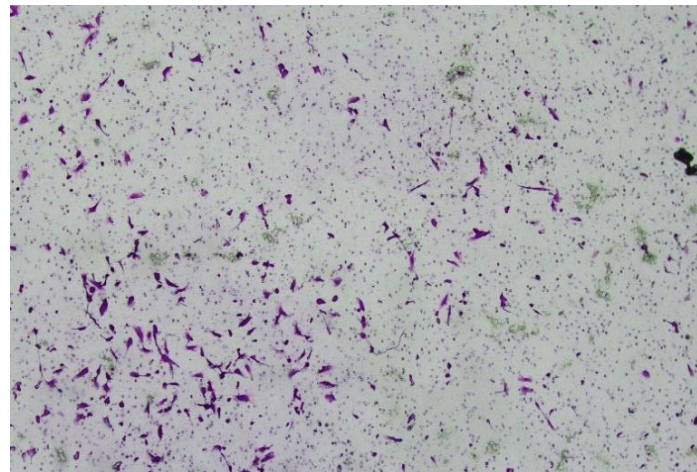
hVEGF



Avastin, 0.5 mg/mL



Cpd-1



Cpd-2

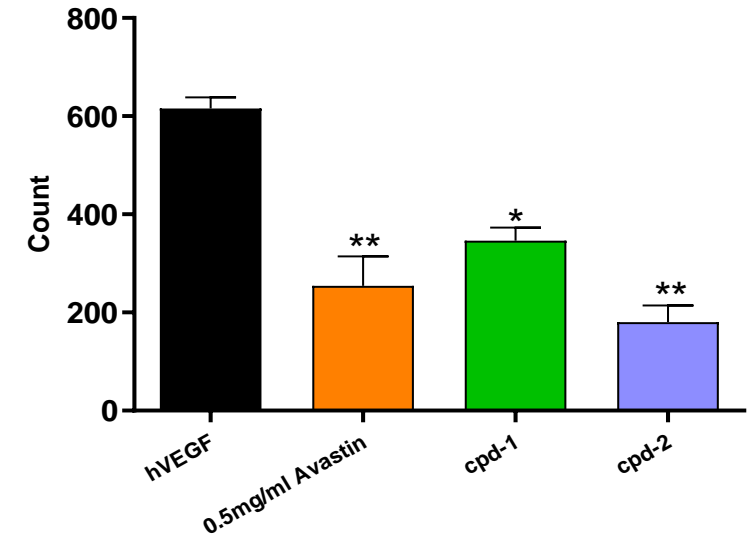
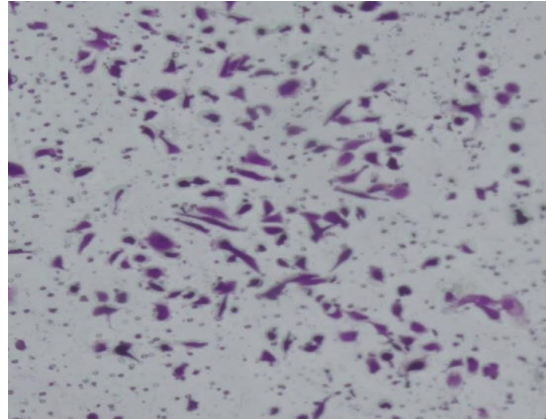


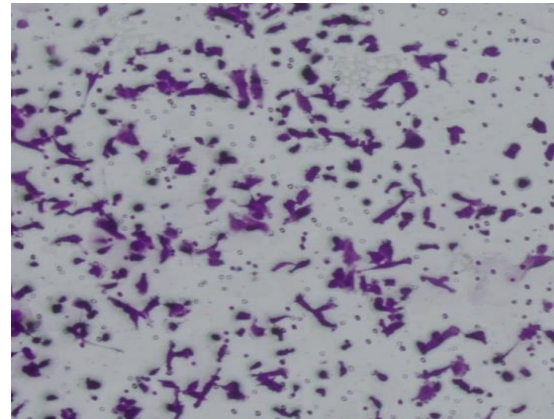
Figure. Cpd-1 and Cpd-2 inhibited the migration of HUVEC cells. HUVEC cells were treated with Cpd-1 and Cpd-2 to evaluate cell migration, 0.5 mg/mL Avastin as control. Data are presented as mean \pm SD from two independent experiments. * $P < 0.05$ vs. hVEGF.

Transwell Invasion Assay

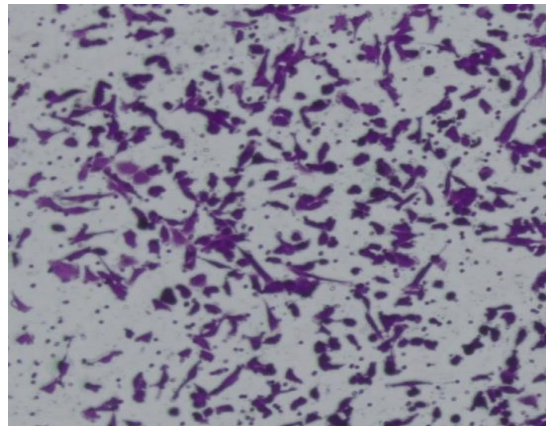
Case study: MDA-MB-231 cell invasion



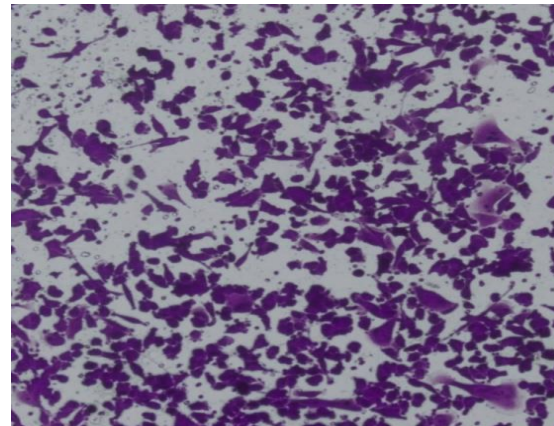
Control



EGF, 40 ng/mL



EGF, 80 ng/mL



EGF, 120 ng/mL

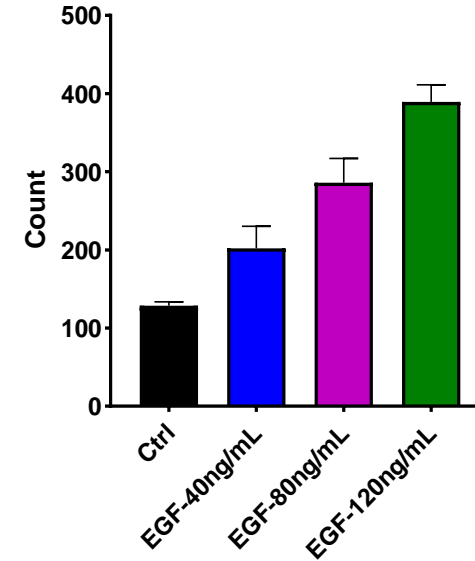
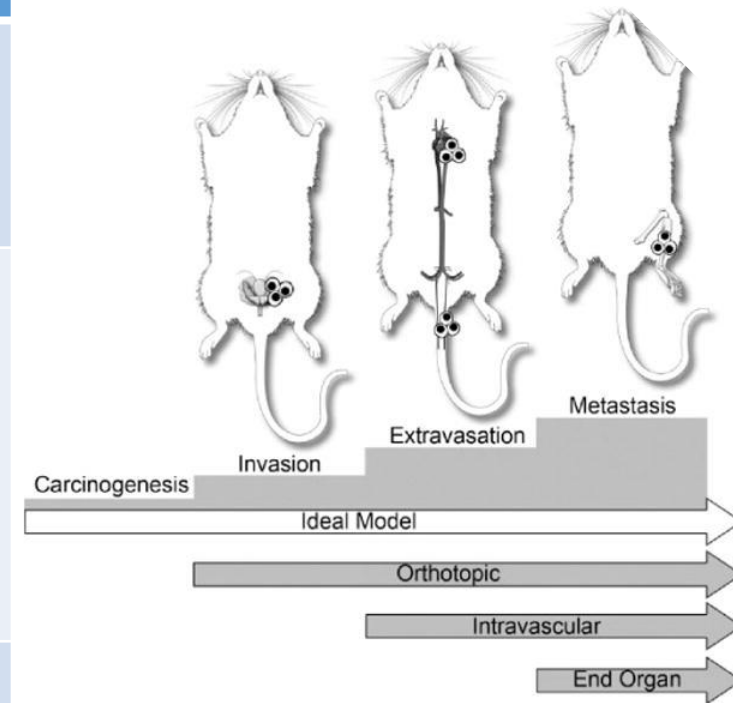


Figure: The invasion of MDA-MB-231 cells. The upper chamber was coated with Matrigel. Then MDA-MB-231 cells were seeded in the upper chamber, and EGF was added to the lower chamber at different concentrations. After 48 hours, the number of cells entering the lower chamber were counted to evaluate the ability of invasion.

Experimental metastasis xenograft models

Strengths and inoculation routes of different models

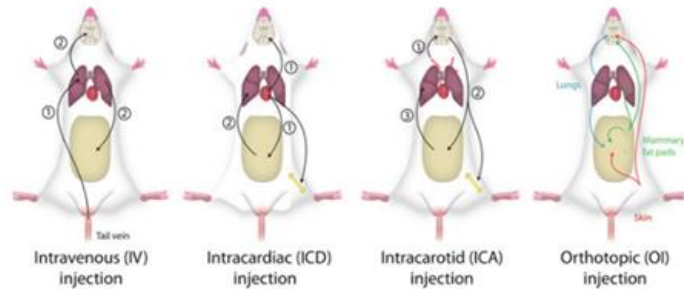
Type of model	Strengths	Inoculation route
Spontaneous metastasis models	<ul style="list-style-type: none"> Metastatic disease development from primary tumor site mimics human disease progression Models all stages of the metastatic cascade Immunocompetent host if allograft Low cost 	<ul style="list-style-type: none"> Orthotopic injection
Experimental metastasis models	<ul style="list-style-type: none"> Rapid and reproducible development of metastases Site-specific development of metastases Applicable to a wide number of cell lines and tumor models Immunocompetent host if allograft Low cost 	<ul style="list-style-type: none"> Ectopic injection (cancer cells are injected to metastasis site) Intra-carotid injection Intra-venous injection Intra-cardiac injection Intra-caudal arterial injection Intra-peritoneal injection Intra-osseous injection
Genetically engineered mouse models	<ul style="list-style-type: none"> Metastatic spread of spontaneous de novo tumors, mimicking human disease Tumors develop in natural microenvironment Tumors display genetic heterogeneity Tumors resemble the molecular and histopathological characteristics of the human disease Models have the potential to model all stages of the metastatic cascade Immunocompetent host 	



Vet Pathol. 2015 September ; 52(5): 827–841.

Experimental brain metastasis xenograft models

37 brain metastasis xenograft models covering 5 tumor types



The route of inoculation will provide different pattern for secondary metastasis

Clin Exp Metastasis. 2013 Jun;30(5):695-710.

Metastatic organ	Tumor type	Cell line	Inoculation site
Brain	Breast (9)	HCC1954-luc ^S , MDA-MB-231-luc-D3H2LN, JIMT-1-luc ^S	Intra-carotid
		xxT47D-luc, MDA-MB-436-luc, xHCC1954/T-DM1-R-Luc1, MDA-MB-231-luc, MCF7-luc, HCC1954-luc	Intra-cranial
	Lung (16)	NCI-H1373-luc, NCI-H1975-luc ^S , NCI-H2228-luc, NCI-H441-luc, NCI-H460-luc2, PC-9-luc ^S , PC-9 EGFR DTC-luc ^S , NCI-H1703-luc, NCI-H2122-luc ^S , LU-01-0426-luc	Intra-cranial
		NCI-H292-luc, NCI-H1373-luc ^S , NCI-H1975-luc ^S , NCI-H2122-luc, PC-9-luc ^S	Intra-carotid
		PC-9-luc	Intra-cardiac
	Melanoma (7)	SK-MEL-3-luc, SK-MEL-5-luc, SK-MEL-24-luc, SK-MEL-28-luc, A375-luc, A375	Intra-cranial
		A375-luc	Intra-carotid
	Pancreas (4)	MIA-PaCa-2-luc, AMG510-R-xMiaPaCa-2-luc, ASPC-1-luc	Intra-cranial
		ASPC-1-luc	Intra-carotid
	Gastric (1)	NCI-N87-Luc	Intra-cranial

S: validated with SOC

Brain metastasis xenograft models established by intra-cranial inoculation

Case study: MDA-MB-231-luc brain metastasis model established by intra-cranial inoculation

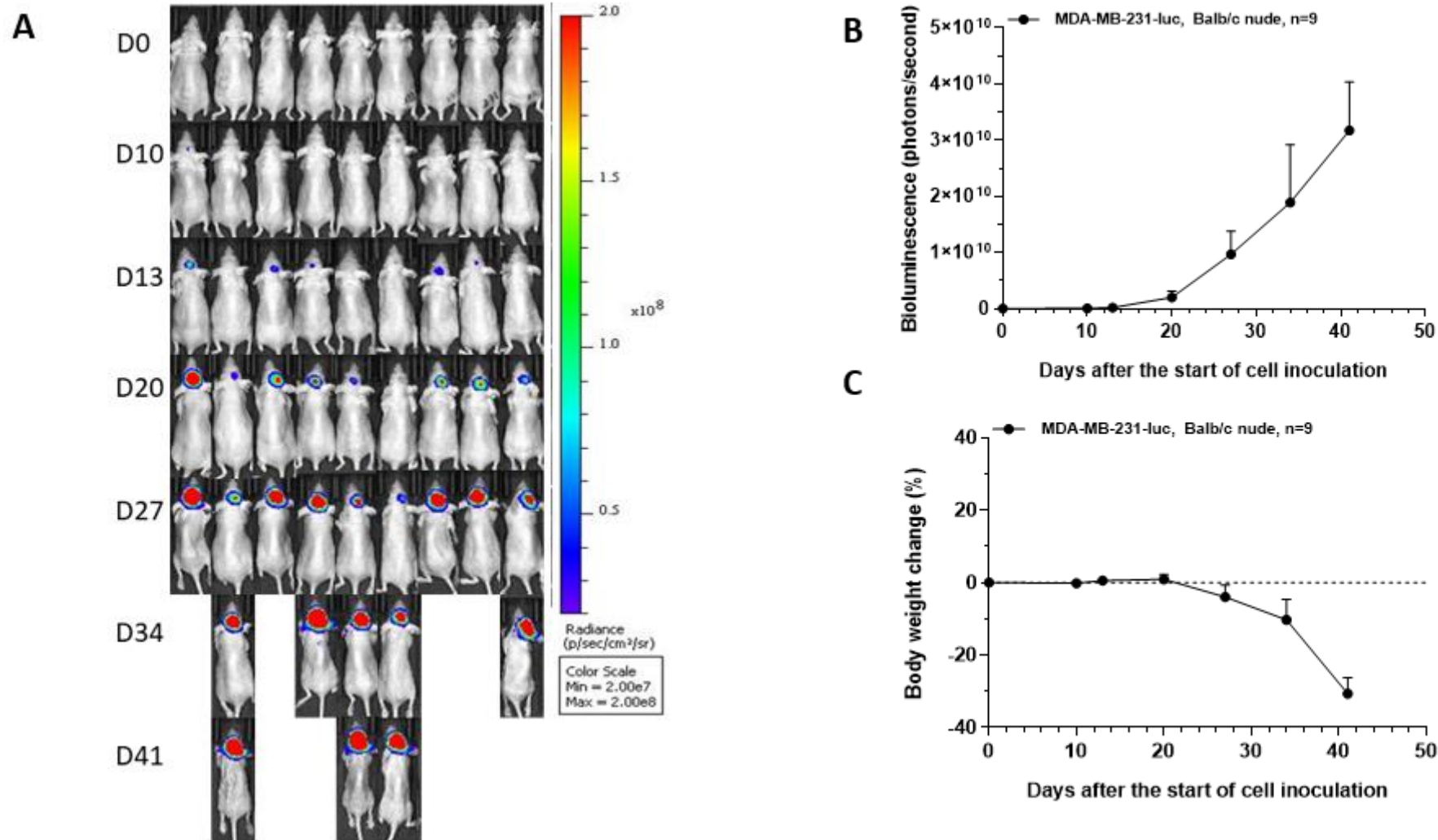


Figure: MDA-MB-231-luc cells were injected into the brain of female Balb/c nude mice **(A)** Bioluminescent imaging of mice over 41 days. **(B)** Metastatic brain tumor growth curve as measured by average relative photon intensity of mice. **(C)** Body weight changes of mice in the experiment.

Brain metastasis xenograft models established by intra-carotid inoculation

Case study: A375-luc brain metastasis model established by intra-carotid inoculation

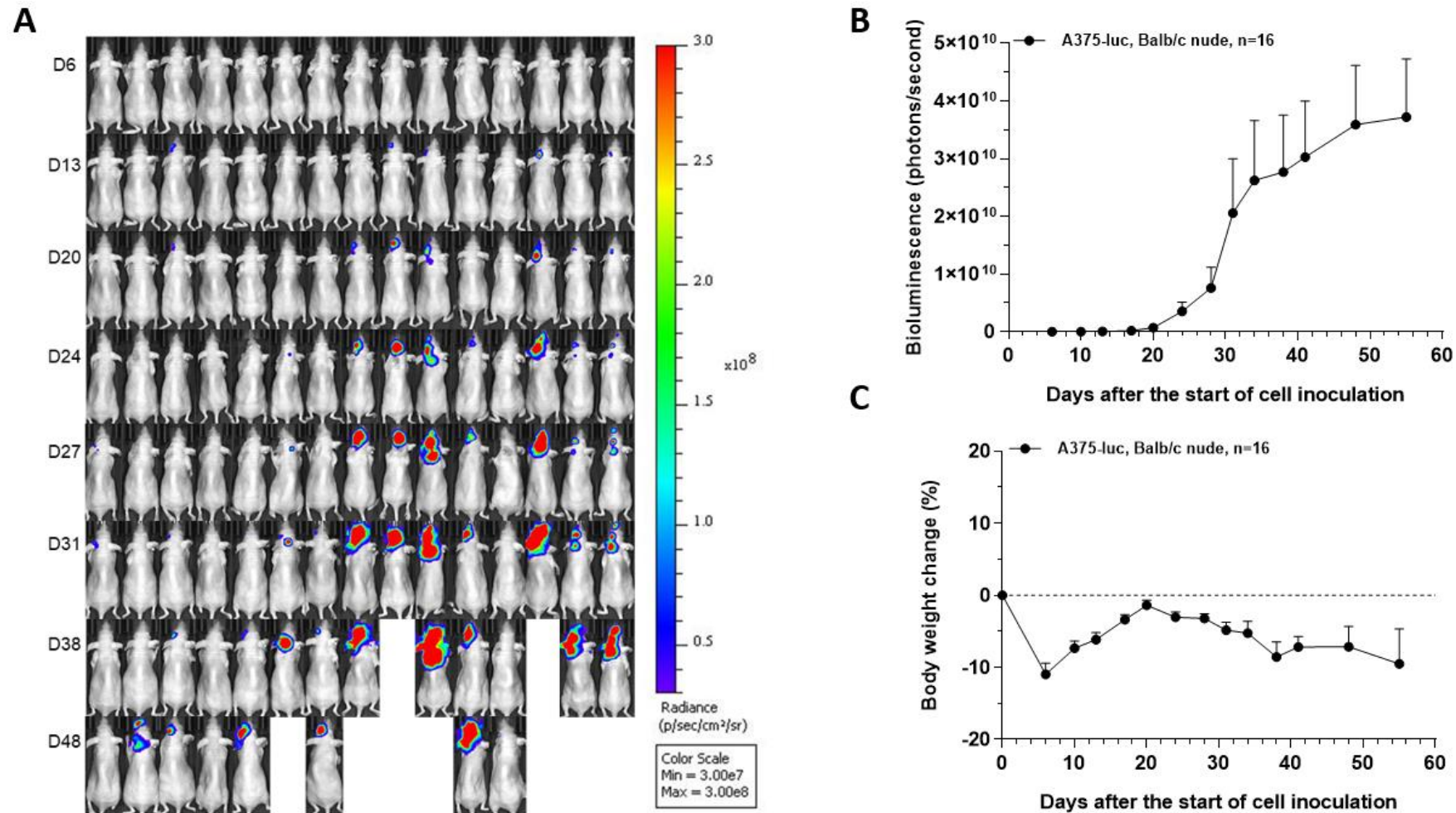


Figure: A375-luc cells were injected into the carotid artery of female Balb/c nude mice. **(A)** Bioluminescent imaging of mice over 48 days. **(B)** Metastatic brain tumor growth curve as measured by average relative photon intensity of mice. **(C)** Body weight changes of mice in the experiment.

Brain metastasis models established by intra-cardiac inoculation

Case study: PC-9-luc brain metastasis model established by intra-cardiac inoculation

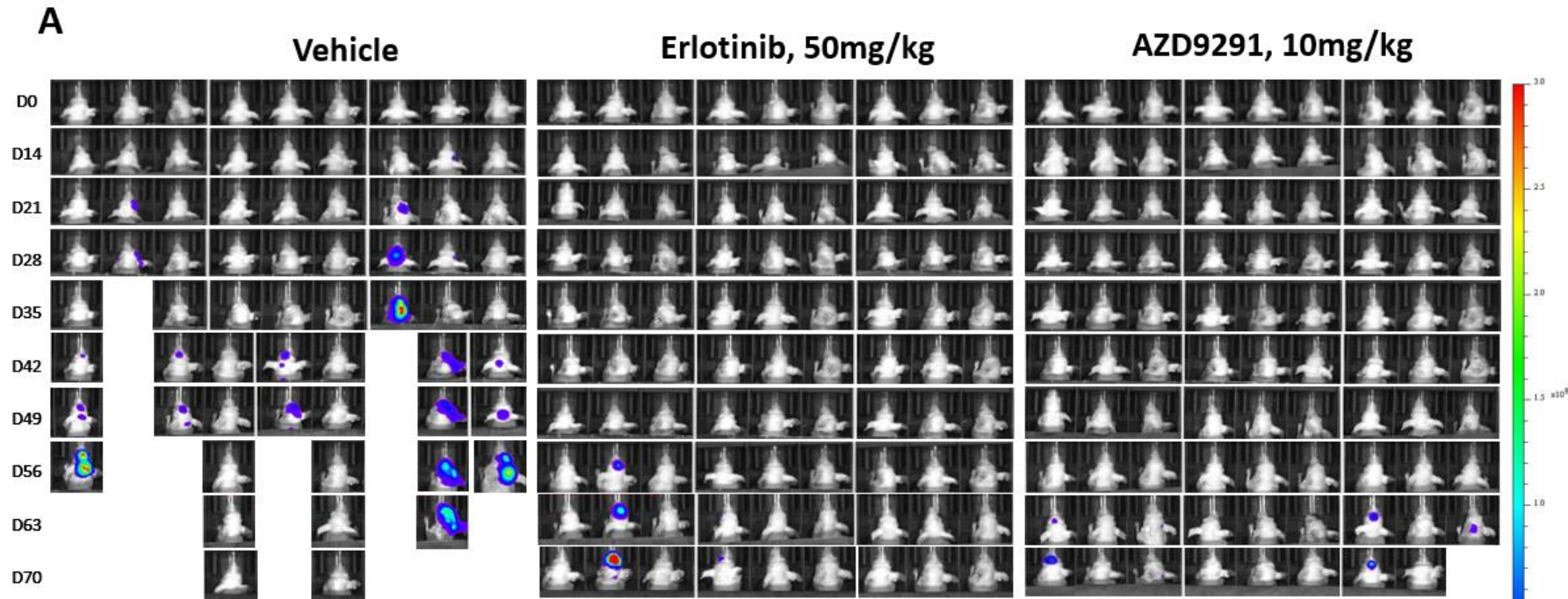
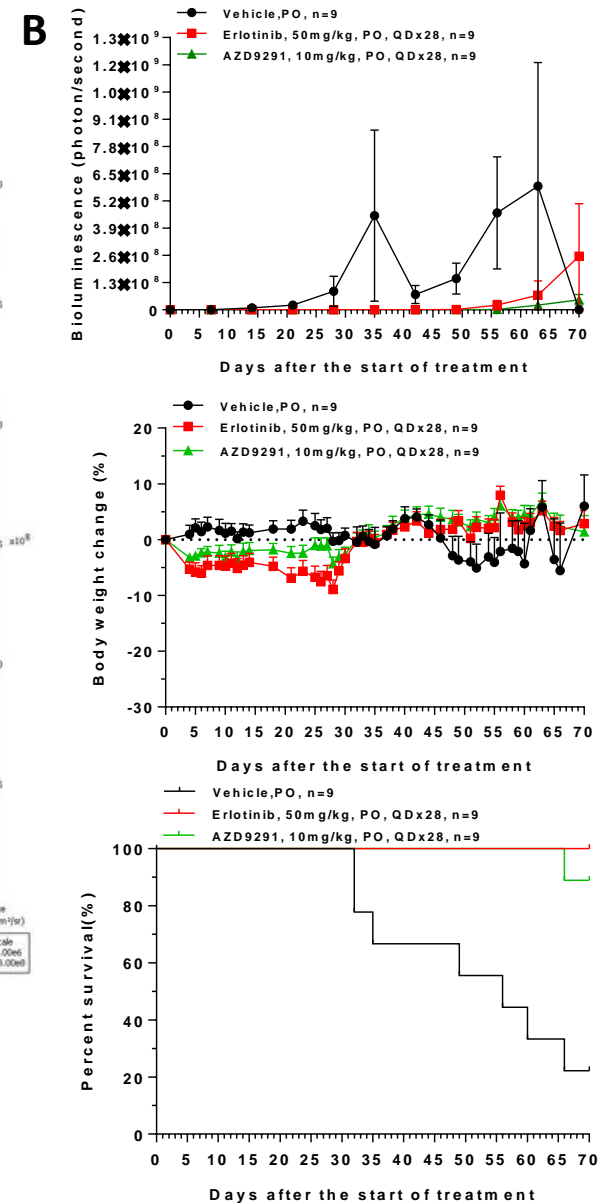
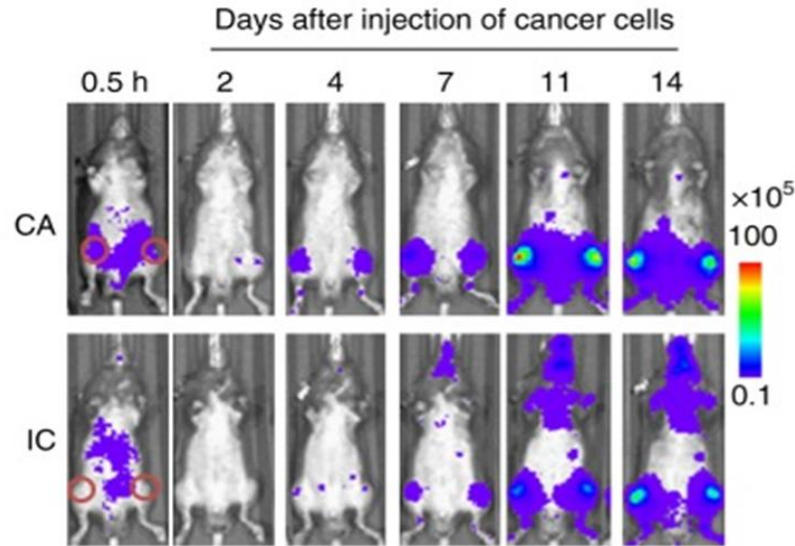


Figure: PC-9-luc cells were injected into the left ventricle of female BALB/c nude mice. **(A)** Bioluminescent imaging of mice over 70 days (n=10). **(B)** Metastatic brain tumor growth curve as measured by average relative photon intensity of mice. **(C)** The average body weight change curve during the experiment. **(D)** Survival curve till day 70.



Experimental bone metastasis xenograft models

14 bone metastasis xenograft models covering 3 tumor types



Intracardiac(IC) /intra-caudal arterial(CA) inoculation: cancer cells can be delivered to bone marrow, and develop bone metastasis eventually.

Nat Commun. 2018; 9: 2981.

Metastatic organ	Tumor type	Cell line	Inoculation site
Bone	Breast (9)	<i>MCF7-luc^S, MDA-MB-231-luc, HCC-1954-Luc</i>	<i>Intra-tibia</i>
		<i>MDA-MB-231-luc</i>	<i>Intra-cardiac</i>
		<i>MCF7-luc^S, JIMT-1-luc-GFP, MDA-MB-231-luc-D3H2LN</i>	<i>Intra-caudal arterial</i>
		<i>MDA-MB-231-luc, MDA-MB-231-luc-D3H2LN</i>	<i>Intra-femur</i>
	Lung (2)	<i>NCI-H358-luc, NCI-H1373-luc</i>	<i>Intra-femur</i>
	Prostate (3)	<i>PC-3M-luc^S</i>	<i>Intra-tibia</i>
		<i>PC-3M-luc</i>	<i>Intra-caudal arterial</i>
		<i>C4-2B-luc</i>	<i>Intra-tibia</i>

S: validated with SOC

Bone metastasis xenograft models established by intra-tibia inoculation

Case study: C4-2B-luc bone metastasis model established by intra-tibia inoculation

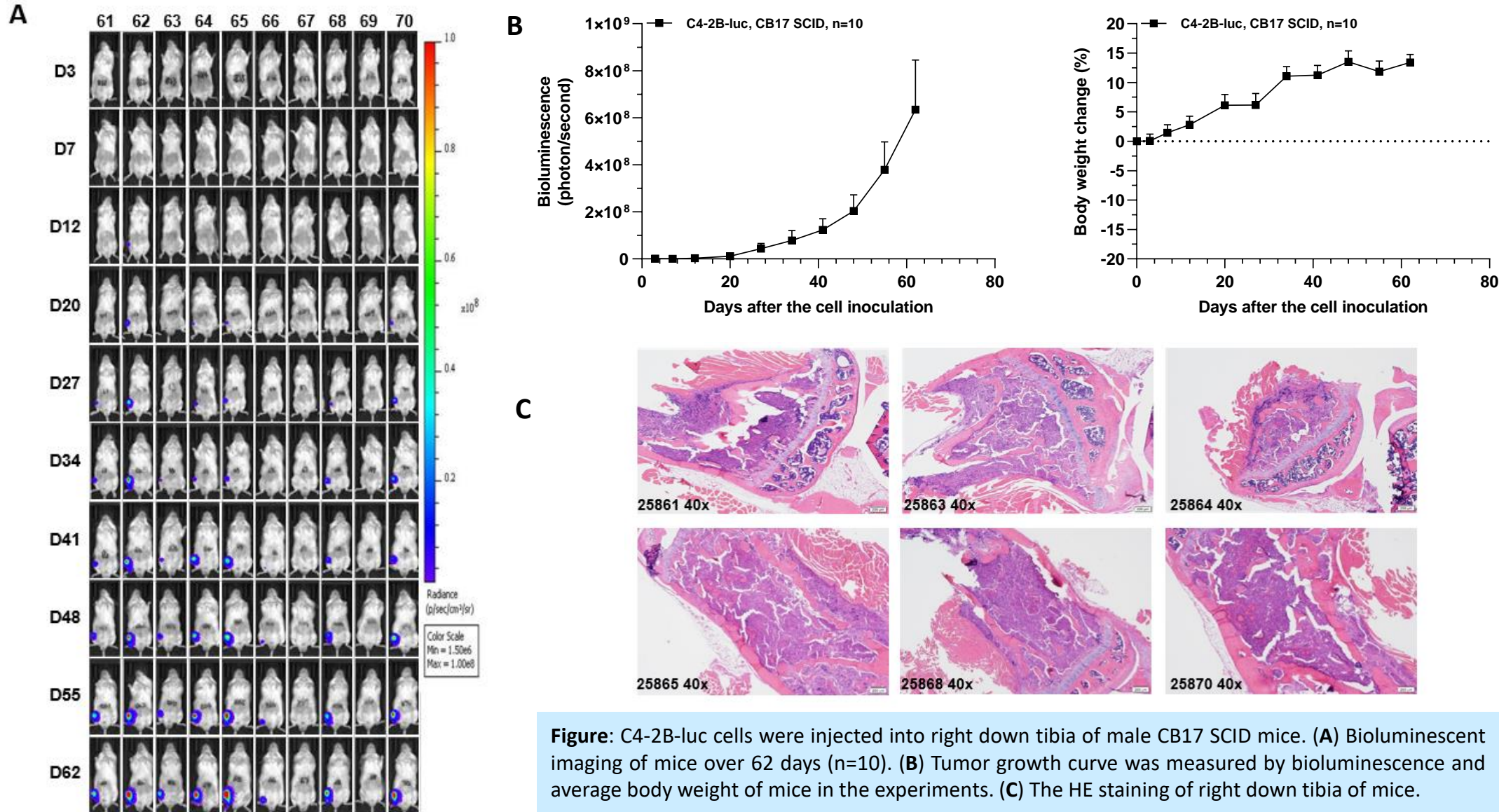


Figure: C4-2B-luc cells were injected into right down tibia of male CB17 SCID mice. **(A)** Bioluminescent imaging of mice over 62 days (n=10). **(B)** Tumor growth curve was measured by bioluminescence and average body weight of mice in the experiments. **(C)** The HE staining of right down tibia of mice.

Bone metastasis xenograft models established by intra-femur inoculation

Case study: NCI-H358-luc bone metastasis model established by intra-femur inoculation

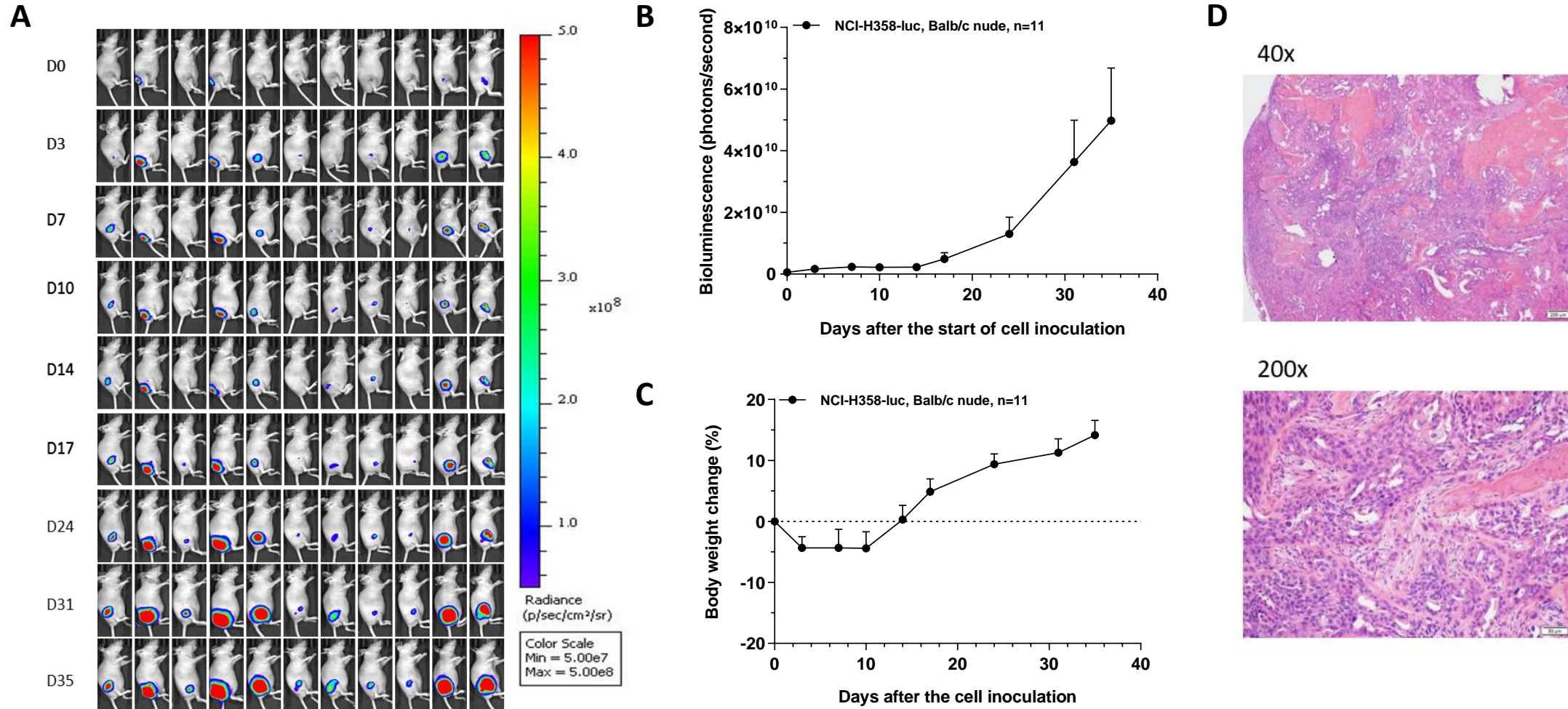


Figure: NCI-H358-luc cells were injected into the femoral cavity of female Balb/c nude. **(A)** Bioluminescent imaging of mice over 35 days. **(B)** Metastatic bone tumor growth curve as measured by average relative photon intensity of mice. **(C)** Body weight changes of mice in the experiment. **(D)** H&E staining of bone lesions showed establishment of bone metastases.

Case study: PC-3M bone metastasis model established by intra-caudal arterial inoculation

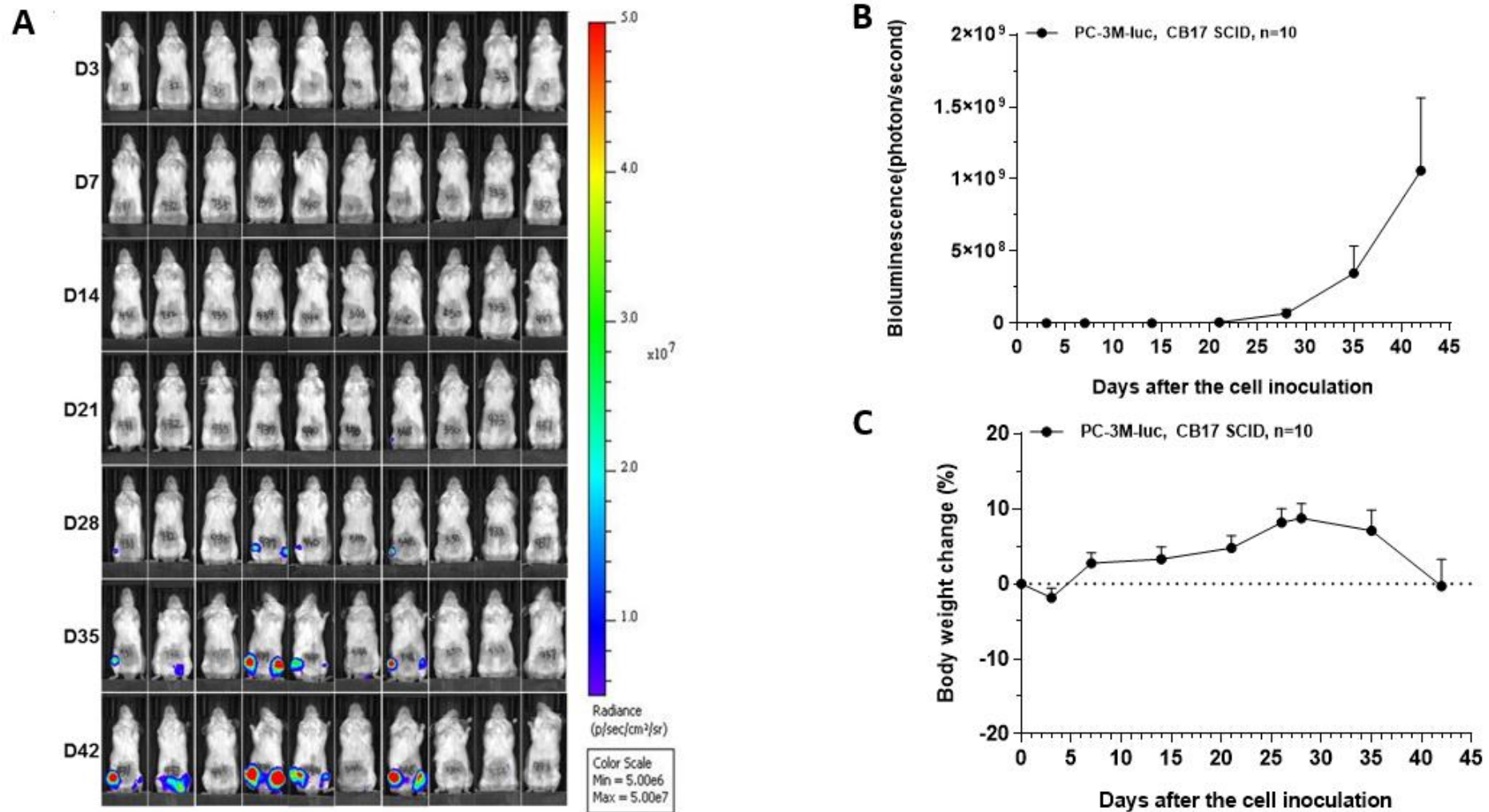


Figure: PC-3M-luc cells were injected into the caudal arterial of male CB17 SCID mice. **(A)** Bioluminescent imaging of mice over 42 days (n=10). **(B)** Tumor growth curve was measured by bioluminescence. **(C)** Body weight growth curve during the experiment.

Bone metastasis xenograft models established by intra-cardiac inoculation

Case study: MDA-MB-231-luc bone metastasis model established by intra-cardiac inoculation

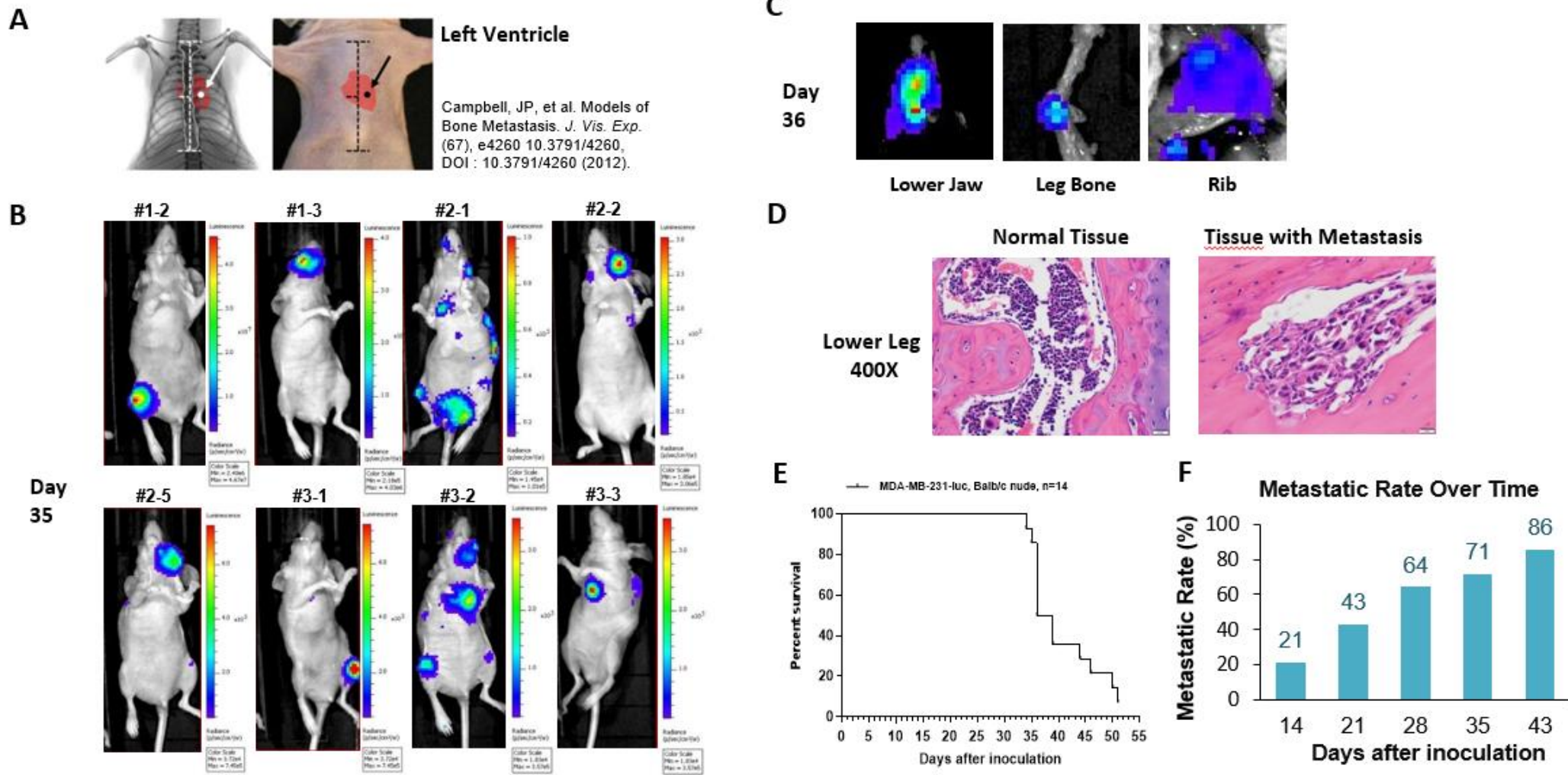
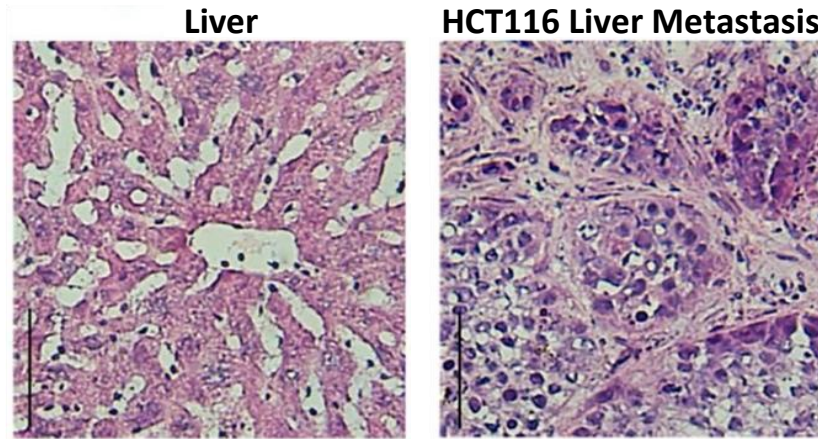
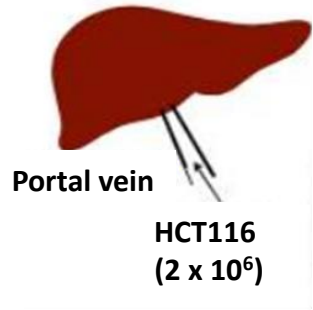


Figure: MDA-MB-231-luc cells were injected into the left ventricle of female BALB/c nude mice. **(A)** Illustration for the injection site. **(B)** Bioluminescent imaging of the mice with bone metastasis. **(C)** ex vivo imaging of the metastatic foci. **(D)** H&E staining of the tissue invaded by metastatic cells. **(E)** Survival curve of inoculated mice (N=14). **(F)** Metastatic rate over time (N=14)

Experimental liver metastasis xenograft models

1 liver metastasis xenograft model



Intraportal inoculation: cancer cells can be delivered firstly and directly to the liver without removal of the spleen.

NPJ Precis Oncol. 2018; 2: 2.

Metastatic organ	Tumor type	Cell line	Inoculation site
Liver	Colon (1)	<i>HCT116-Luc</i>	<i>hepatic portal vein</i>

Liver metastasis xenograft models established by intraportal inoculation

Case study: HCT116-luc liver metastasis model established by intraportal inoculation

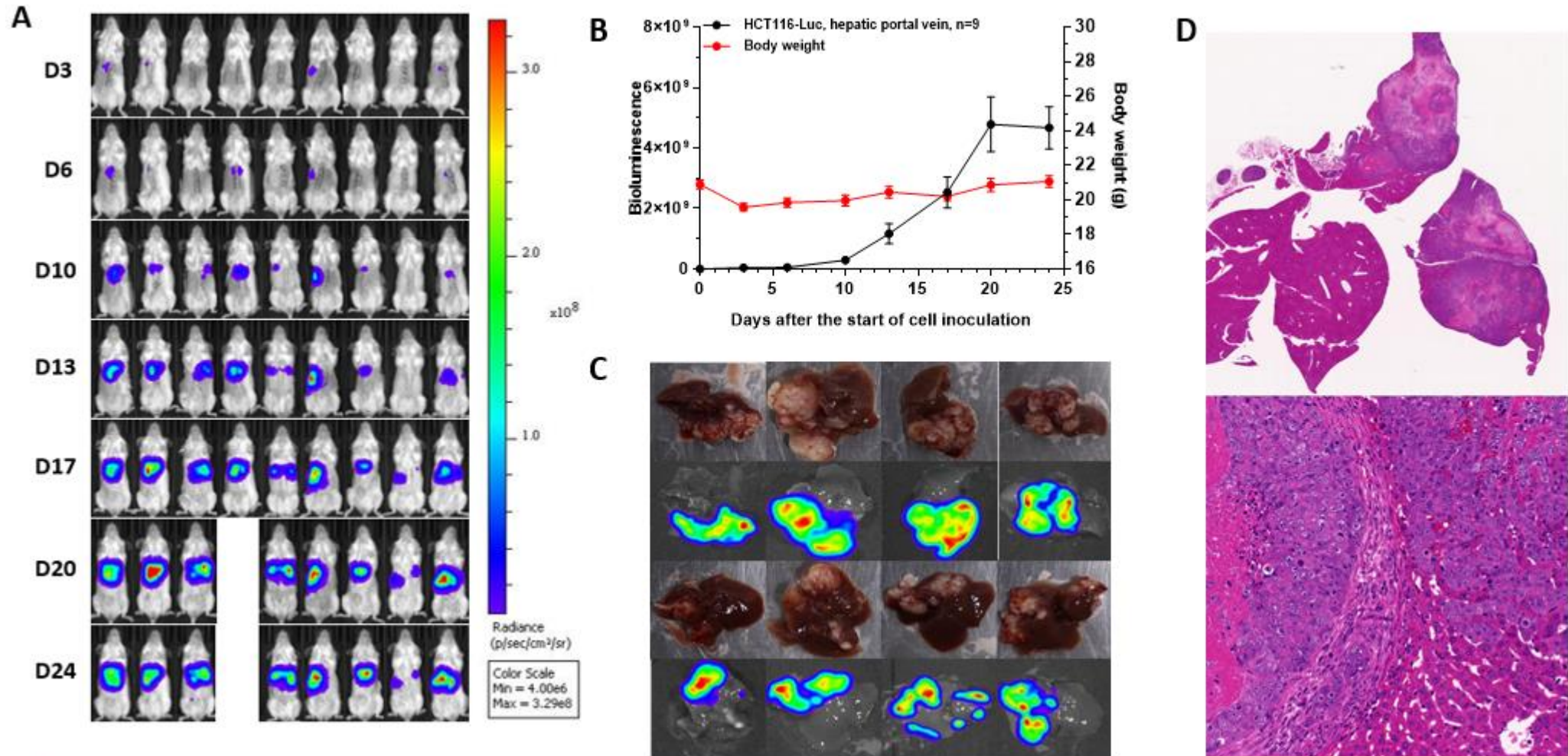
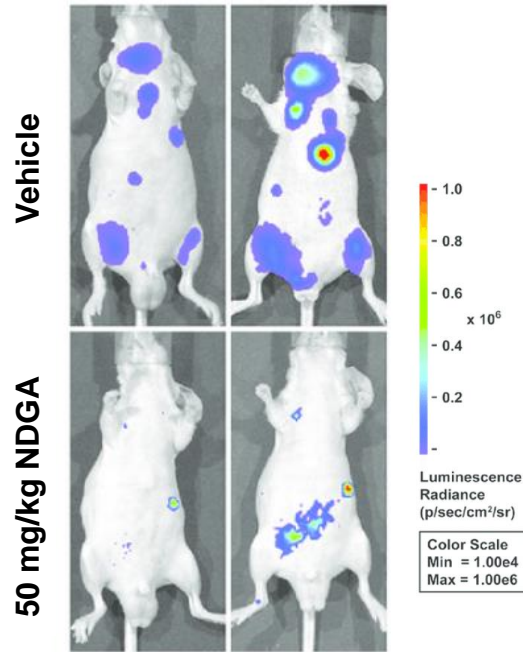


Figure: HCT116-luc cells were injected into NOD SCID mice via the hepatic portal vein. **(A)** Bioluminescent imaging of mice over 24 days (n=9). **(B)** Tumor growth curve was measured by average relative photon intensity and bodyweight of mice in the experiment. **(C)** The photo and bioluminescence of liver bearing tumor. **(D)** H&E staining of liver tissue showed establishment of hepatic metastases

Disseminated xenograft models

8 disseminated xenograft models covering 3 tumor types



Intravenous (IV) inoculation: The tumor cells will be disseminated to the lungs, brain and other organs of the body.

Oncotarget. 2016; 7:86225-86238

Metastatic organ	Tumor type	Cell line	Inoculation site
Multiple organs	Brain (1)	<i>SK-N-SH-luc</i>	<i>Intra-venous</i>
	Breast (5)	<i>JIMT-1-luc, MDA-MB-231-luc, MDA-MB-436-luc, HCC-1806-Luc, HCC-1954-Luc</i>	<i>Intra-venous</i>
	Lung (2)	<i>NCI-H292-luc, HCC827-Luc</i>	<i>Intra-venous</i>

Disseminated xenograft models established by intra-venous inoculation

Case study: JIMT-1-luc disseminated xenograft model established by intra-venous inoculation

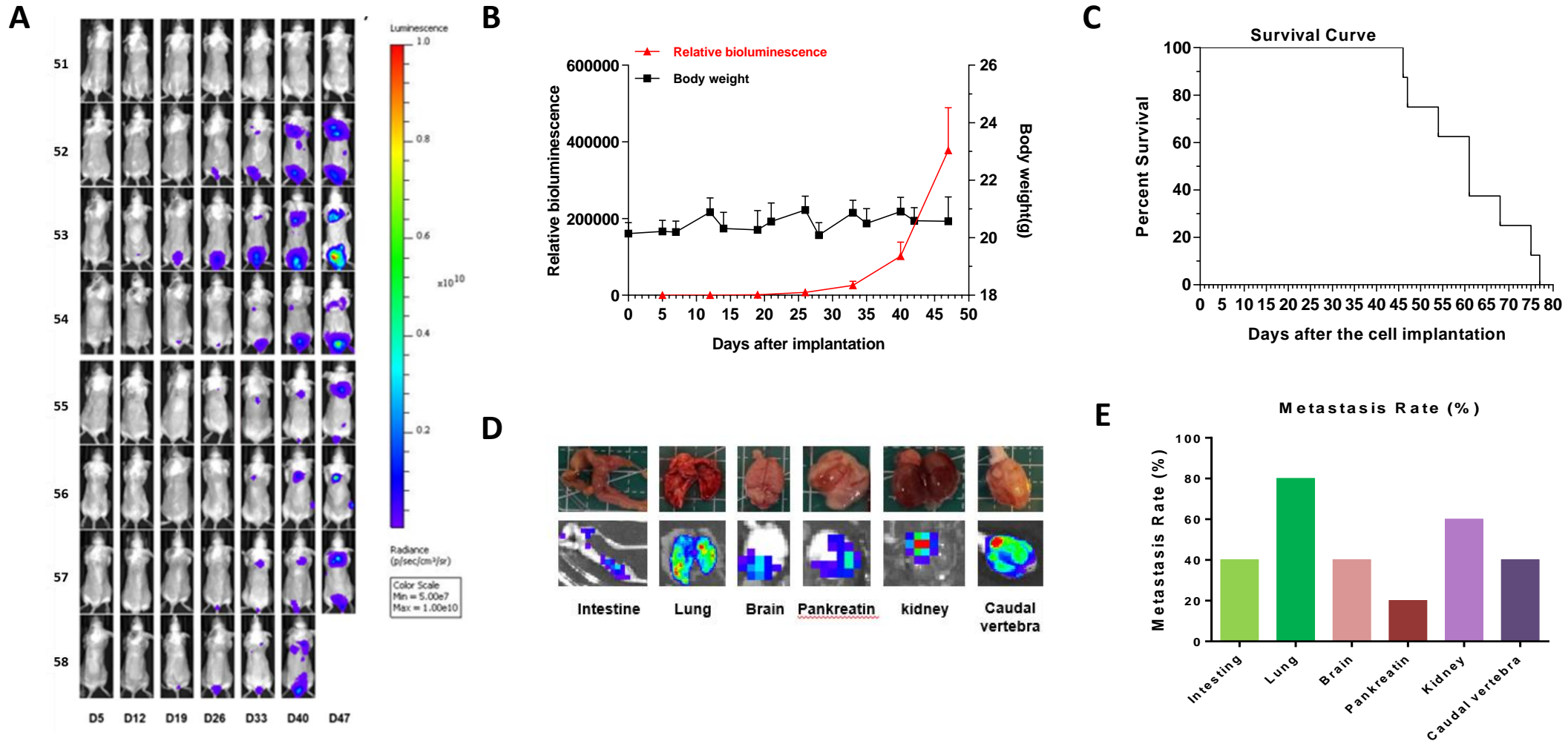
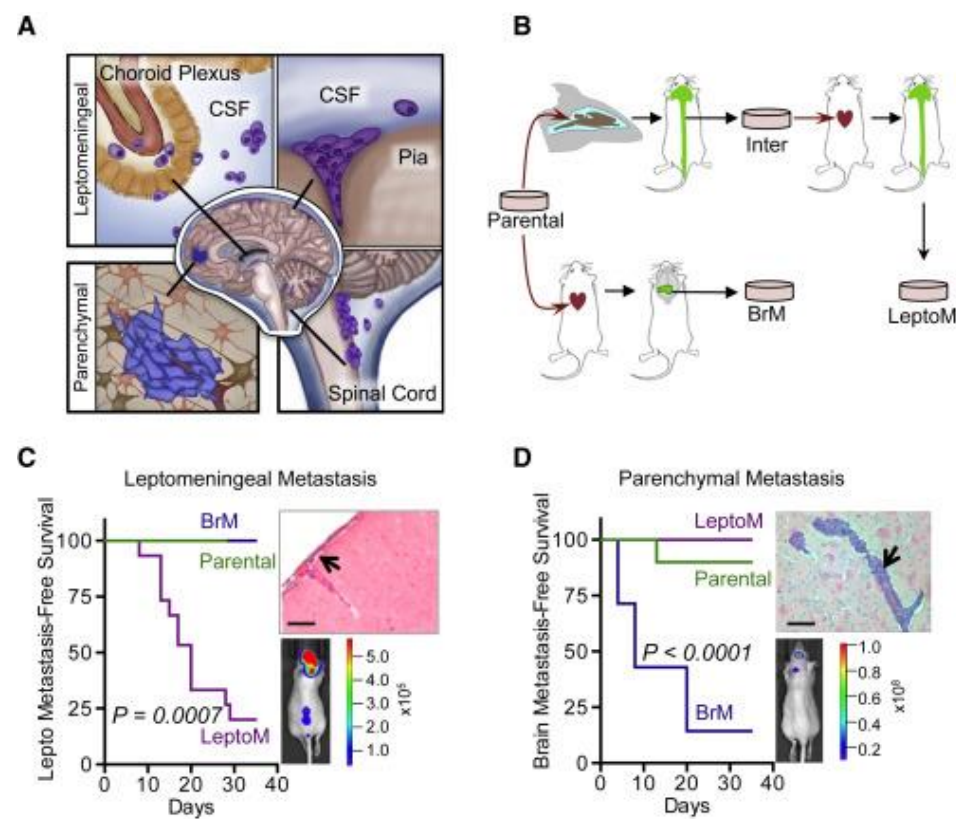
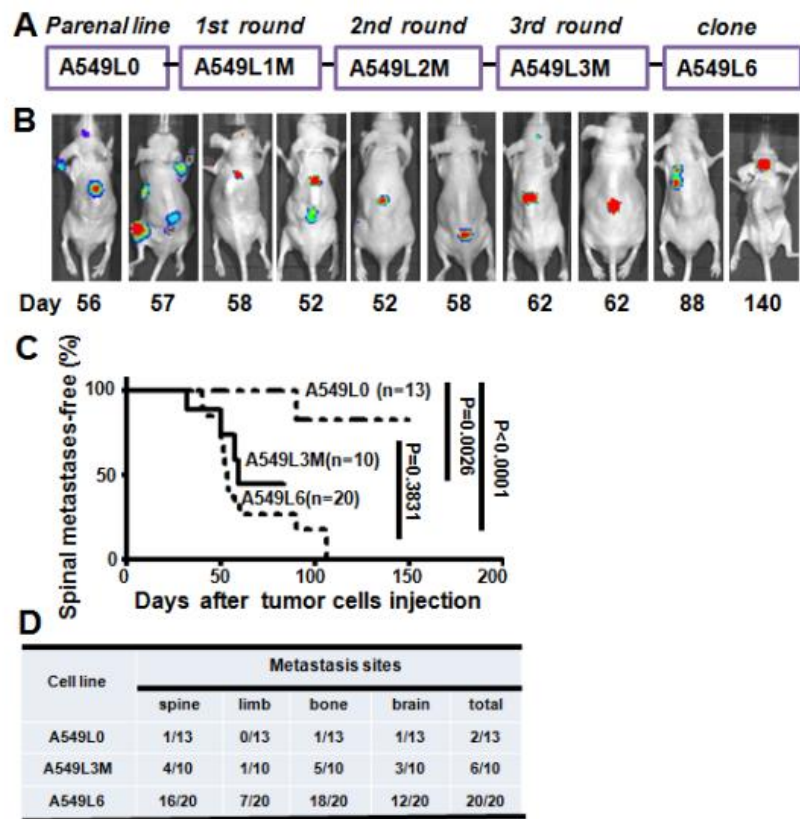


Figure: JIMT-1-luc cells were injected into the vein of SCID Beige mice. **(A)** Bioluminescent imaging of mice over 47 days (n=8). **(B)** Tumor growth curve as measured by average relative photon intensity in the experiments and the average body weight curve of mice was used in the experiment. **(C)** survival curve during the period. **(D)** Anatomical and bioluminescence image of the metastatic organs. **(E)** The metastasis rate of this model.

Background

In vivo selection has proven an effective approach to isolate organ-specific metastatic subpopulations from heterogeneous cancer cell lines. Generally, cell lines labeled with luciferase or other tags are inoculated into immuno-deficient mice. Tumor cells are extracted from targeted organ and cultured *in vitro* for expansion, then reinoculated into mice. After several rounds of *in vivo* selection, organ-specific metastatic cell lines will be obtained.



Oncotarget. 2015 Sep 8;6(26):22905-17.

Cell. 2017 Mar 9;168(6):1101-1113.e13.

Case study: Establishment of brain-specific metastatic PC-9 cell line

Establishment of *in vivo* selected “brain-seeking” PC-9-BR cell line

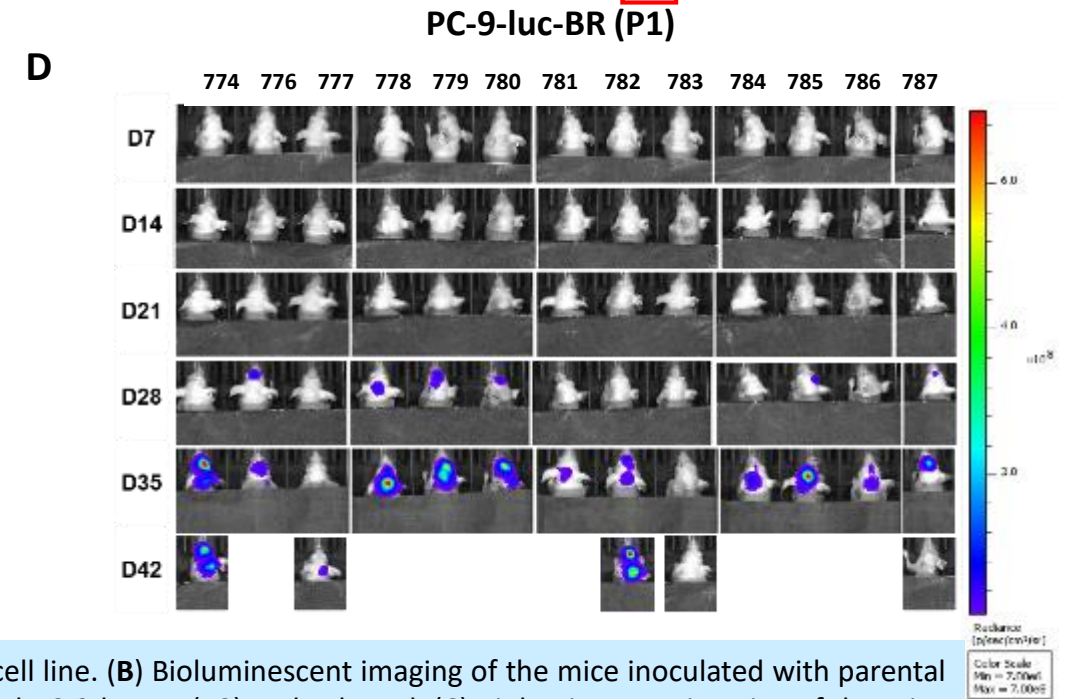
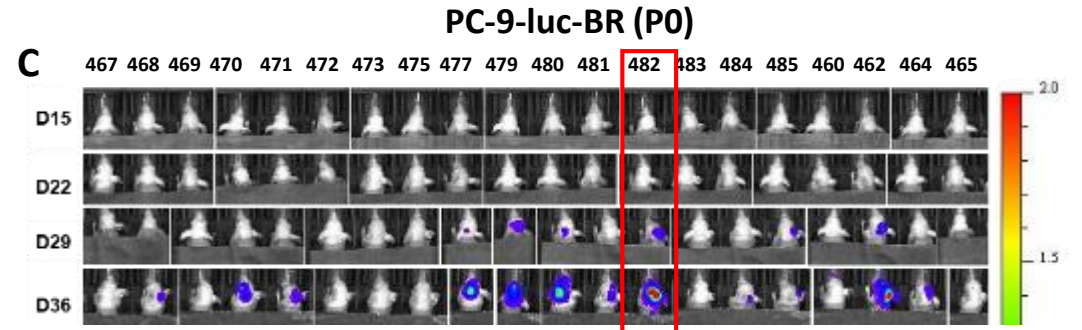
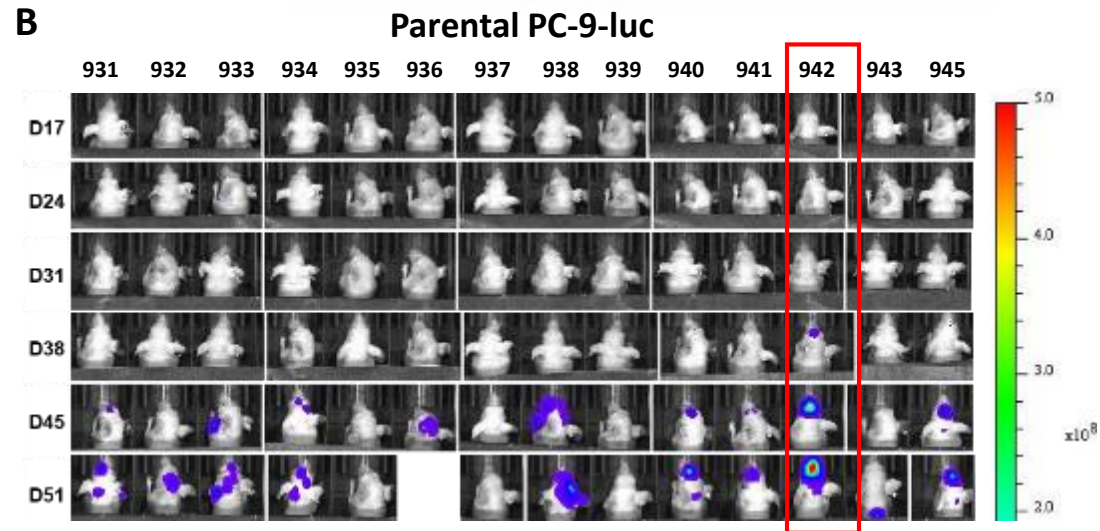
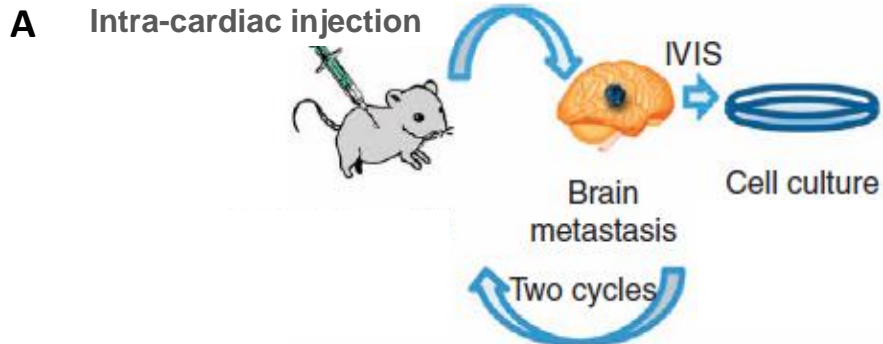
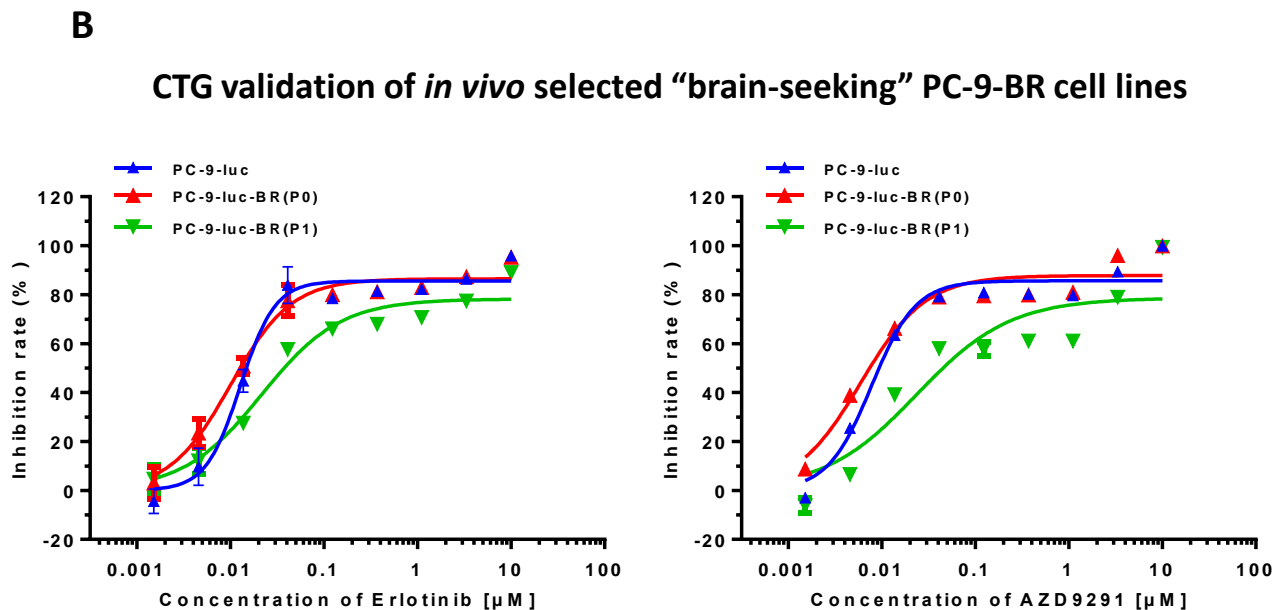
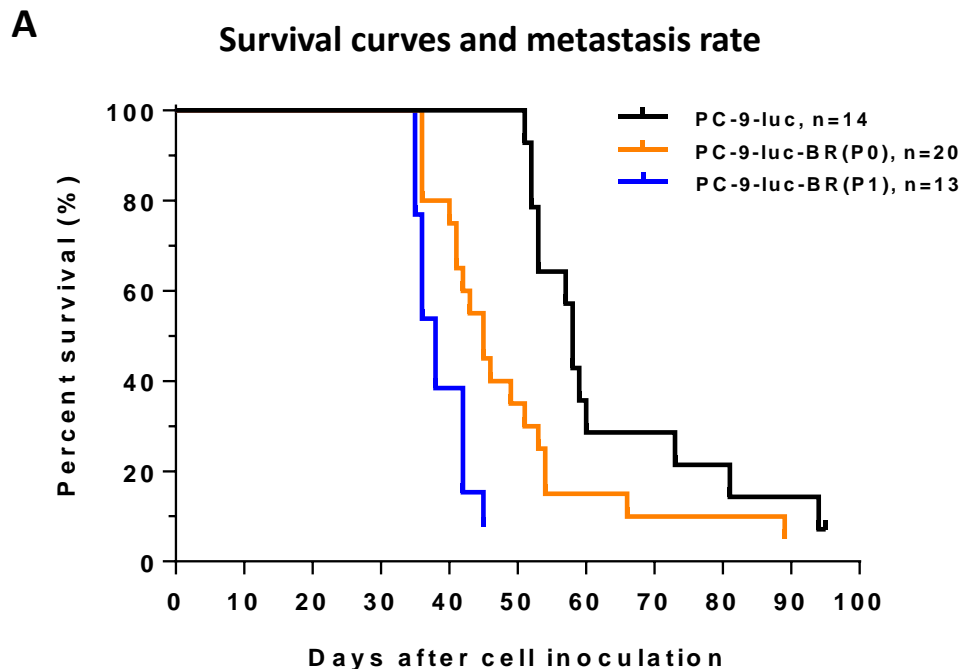


Figure: (A) Illustration for establishment of *in vivo* selected “brain-seeking” PC-9-BR cell line. (B) Bioluminescent imaging of the mice inoculated with parental PC-9-luc cells by intra-cardiac injection. The tumor cells from animal #942 was named PC-9-luc-BR (P0) and cultured. (C) Bioluminescent imaging of the mice inoculated with PC-9-luc-BR (P0) cells by intra-cardiac injection. The tumor cells from animal #482 was named PC-9-luc-BR (P1) and cultured. (D) Bioluminescent imaging of the mice inoculated with PC-9-luc-BR (P1) cells by intra-cardiac injection.

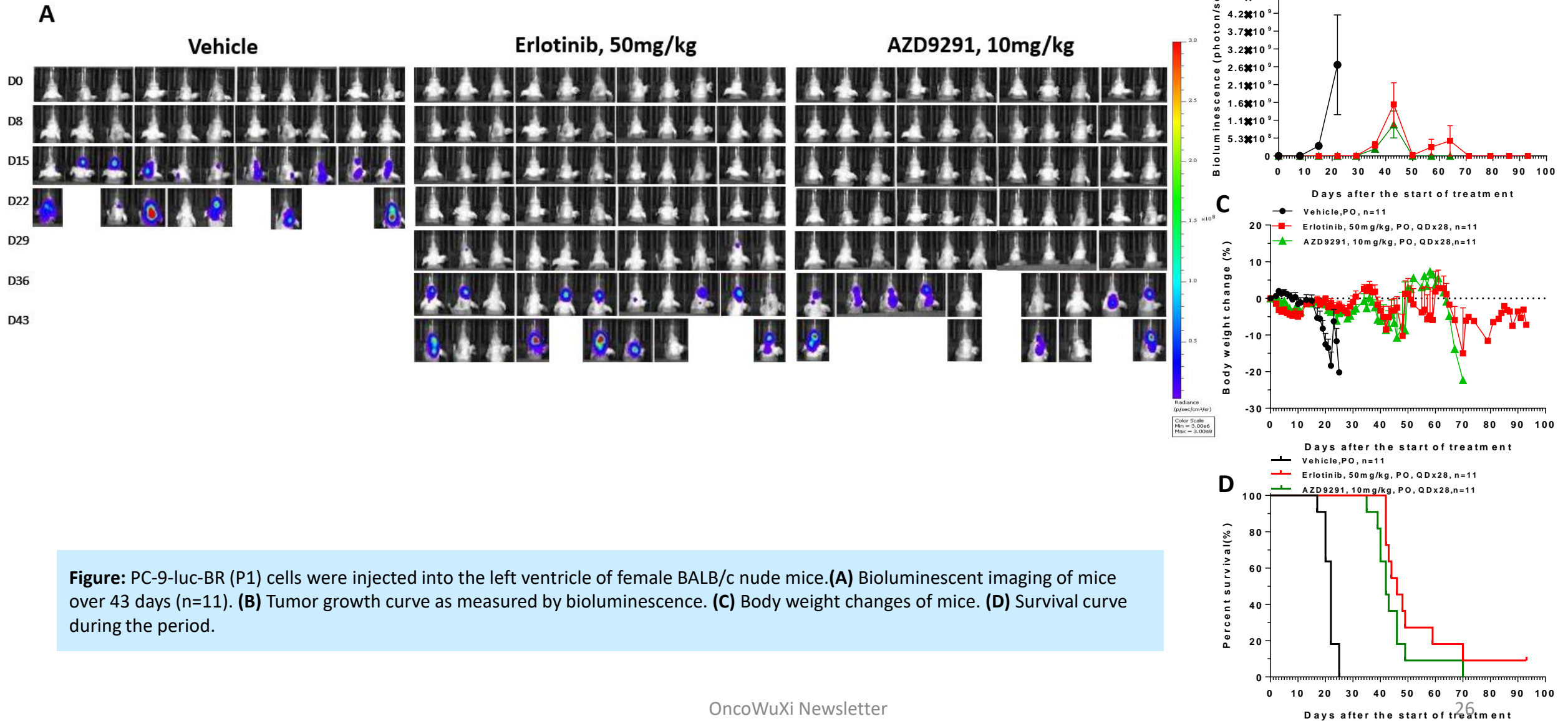


Model	Brain metastasis rate (%)	Other sites metastasis rate (%)	Median survival (day)
PC-9-luc	57	64	58
PC-9-luc-BR (P0)	75	20	45
PC-9-luc-BR (P1)	85	15	38

By *in vivo* selection, brain-specific metastatic PC-9 cell line was established and named PC-9-luc-BR. PC-9-luc-BR (P1) has higher brain metastasis rate than parental PC-9-luc, but shows similar reaction to Erlotinib and AZD9291. RNASeq of PC-9-luc-BR (P1) has also been completed.

Organ-specific metastasis xenograft models established by *in vivo* selection

Case study: Establishment of brain-specific metastatic PC-9 cell line





OUR COMMITMENT

Improving Health. Making a Difference.

For questions and requests, please email to OIU-BD-Translation@wuxiapptec.com



<https://onco.wuxiapptec.com>